ARTICLE

Theoretical Studies on Mechanism and Rate Constant of Gas Phase Hydrolysis of Glyoxal Catalyzed by Sulfuric Acid

Ming-qiang Huang[a,b,c*], Shun-you Cai[a,b], Ying-min Liao[c], Wei-xiong Zhao[d], Chang-jin Hu[d], Zhen-ya Wang[d], Wei-jun Zhang[d*]

a. College of Chemistry and Environment, Minnan Normal University, Zhangzhou 363000, China
b. Fujian Province Key Laboratory of Modern Analytical Science and Separation Technology, Zhangzhou 363000, China
c. Department of Environmental Science and Engineering, College of Tan Kah Kee, Xiamen University, Zhangzhou 363105, China
d. Laboratory of Atmospheric Physico-Chemistry, Anhui Institute of Optics and Fine Mechanics, Chinese Academy of Sciences, Hefei 230031, China

(Dated: Received on September 21, 2015; Accepted on December 4, 2015)

The gas phase hydration of glyoxal (HCOCHO) in the presence of sulfuric acid (H_2SO_4) were studied by the high-level quantum chemical calculations with M06-2X and CCSD(T) theoretical methods and the conventional transition state theory (CTST). The mechanism and rate constant of the five different reaction paths are considered corresponding to HCOCHO+H_2O, HCOCHO+$H_2O\cdots H_2O$, HCOCHO$\cdots H_2O$+H_2O, HCOCHO+$H_2O\cdots H_2SO_4$ and HCOCHO$\cdots H_2O$+H_2SO_4. Results show that H_2SO_4 has a strong catalytic ability, which can significantly reduce the energy barrier for the hydration reaction of glyoxal. The energy barrier of hydrolysis of glyoxal in gas phase is lowered to 7.08 kcal/mol from 37.15 kcal/mol relative to pre-reactive complexes at the CCSD(T)/6-311++G(3df, 3pd)//M06-2X/6-311++G(3df, 3pd) level of theory. The rate constant of the H_2SO_4 catalyzed hydrolysis of glyoxal is 1.34×10^{-11} cm^3/(molecule·s), about 10^{13} higher than that involving catalysis by an equal number of water molecules, and is greater than the reaction rate of glyoxal reaction with OH radicals of 1.10×10^{-11} cm^3/(molecule·s) at the room temperature, indicating that the gas phase hydrolysis of glyoxal of H_2SO_4 catalyst is feasible and could compete with the reaction glyoxal+OH under certain atmospheric conditions. This study may provide useful information on understanding the mechanistic features of inorganic acid-catalyzed hydration of glyoxal for the formation of oligomer.

Key words: Glyoxal, Hydrolysis, Sulfuric acid, Acid-catalyzed mechanism

I. INTRODUCTION

Glyoxal (HCOCHO), which is produced via gas phase photochemical oxidation of biogenic and anthropogenic precursors such as isoprene and aromatics, is the most abundant α-dicarbonyl in the atmosphere [1–4]. The primary removal processes for glyoxal are thought to be photolysis and reaction with OH radicals [5, 6]. Glyoxal is also scavenged by aqueous aerosol, fog, and cloud droplets in the atmosphere due to its high effective Henry's law constant [7–10]. Subsequent aqueous-phase OH oxidation of the dissolved glyoxal can lead to the formation of less volatile products with highly oxygenated organics such as glyoxylic and oxalic acids, and secondary organic aerosol (SOA) upon droplet evaporation [11–13]. In addition to the aqueous-phase OH oxidation mechanisms for producing less volatile products, the reaction between glyoxal and water produces glyoxal-diol ($HCOCH(OH)_2$) is also known as the monohydrated form of glyoxal. Glyoxal-diol can undergo self- and cross-oligomerization to produce dimmers, trimers, and polymers as shown in Fig.1 [8, 10, 14].

In contrast, the gas phase hydrolysis of glyoxal to form glyoxal-diol has not yet been considered in atmosphere because it is commonly believed that there is a substantial barrier to make the hydrolysis energetically feasible [15, 16]. Kua *et al.* [17] used density functional theory (B3LYP/6-311+G*) calculations to show that if only one water included in the transition state, results in a four center transition state with activation energy of 37.0 kcal/mol, that is too large for efficient glyoxal-diol formation under typical atmospheric conditions. However, some studies have demonstrated that atmospheric acids are able to lower the barrier of the gas phase hydrolysis of aldehyde compounds [18–20]. Long *et al.* [18] and Hazar *et al.* [19] have demonstrated that

*Authors to whom correspondence should be addressed. E-mail: wjzhang@aiofm.ac.cn, huangmingqiang@gmail.com

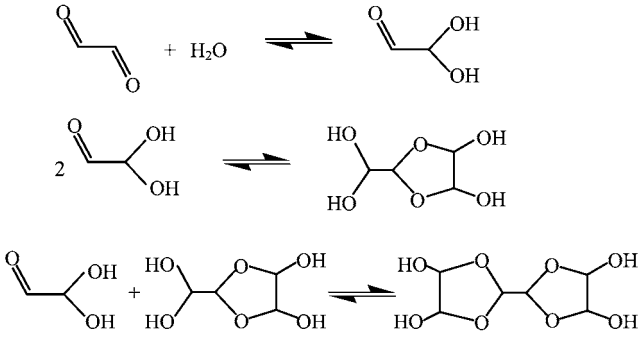

FIG. 1 Proposed reaction mechanisms of hydration, oligomerization for glyoxal.

the ability of sulfuric acid and formic acid effectively catalyze the hydrolysis of formaldehyde to form methanediol, respectively. Very recently, the gas phase hydrolysis of glyoxal involving one to three water molecules and also in the presence of a water molecule and formic acid has been investigated theoretically with MP2/6-311++G(3df, 3pd) by Hazar *et al.* [21]. Their results show that glyoxal-diol is the major product of the hydrolysis and that formic acid, through its ability to facilitate intermolecular hydrogen atom transfer, is considerably more efficient than water as a catalyst in the hydrolysis process.

To the best of our knowledge, no investigations on the gas phase hydrolysis of glyoxal catalyzed by inorganic acids which are present in the atmosphere at significant trace levels are performed up to now. Principal candidates for inorganic acid catalysts are hydrochloric acid (HCl), nitric acid (HNO_3), and sulfuric acid (H_2SO_4), especially H_2SO_4, which is produced through oxidation processing of SO_2 emitted from fossil fuel combustion [22, 23]. In this study, the hydrolysis of HCOCHO catalyzed by H_2SO_4, and water dimer is studied using quantum chemical calculations and conventional transition state theory (CTST) with Eckart tunneling correction to determine whether the gas phase hydrolysis of glyoxal is feasible and important in the atmosphere. This study may provide useful information on understanding the mechanistic features of inorganic acid-catalyzed hydration of glyoxal for the formation of oligomer.

II. COMPUTATIONAL METHODS

As pointed out by Long *et al.* [18] and Elm *et al.* [24], M06-2X functional with the 6-311++G(3df, 3pd) basis set can obtain more reliable results than other functionals for the reaction of atmospheric prenucleation clusters. So, the structures and harmonic vibration frequencies of reactants, complexes, transition states and products were accomplished with the Gaussian 09 software package [25] using the M06-2X/6-311++G(3df, 3pd) level of theory. Additionally, the intrinsic reaction coordinate (IRC) approach [26] was performed to ensure that the given transition state connects with the corresponding reactants and products. Furthermore, single-point energies of optimized geometries were refined using the CCSD(T) theoretical method [27] with the 6-311++G(3df, 3pd) basis set to represent the improved results.

The conventional transition state theory (CTST) [28–31] combined with Eckart correction [32] was employed to investigate the rate constant of every elementary reaction. This method can provide reliable data, which is extensively utilized in the atmospheric reactions [18, 33–35]. They were computed using the Eckart method implemented in TheRate 1.1 program [36] which is provided in the csed.net web site. According to the steady-state conditions [30], the reactions begin with the formation of the pre-reactive complexes before the transition sates:

$$\text{Reactant} \xleftrightarrow{K_{\rm eq}} \text{Pre-reactive complex} \xleftrightarrow{k_2} \text{Products}$$

The total rate constant $k(T)$ is formulated as:

$$k = K_{\rm eq} k_2$$

where $K_{\rm eq}$ and k_2 are the equilibrium constant of the first step and the rate constant of the second step in the reactions, respectively.

III. RESULTS AND DISCUSSION

A. Hydrolysis of glyoxal catalyzed by water

Similar to the gas phase hydrolysis of formaldehyde proposed by Hazar *et al.* [19], the hydrolysis of glyoxal involving one water molecule can be considered as follows:

$$\begin{aligned} \mathrm{HCOCHO + H_2O} &\xleftrightarrow{K_{\rm eq1}} \mathrm{HCOCHO\cdots H_2O} \ \text{(C1)} \\ &\xrightarrow{k_{21}} \mathrm{HCOCH(OH)_2} \end{aligned} \tag{1}$$

The above reaction has been recently studied by Kua *et al.* [17] and Hazar *et al.* [21]. Their results indicated that the interaction between glyoxal and water can form several geometries that basically differ with respect to the relative orientation of the water and glyoxal subunits. The geometries of various $\mathrm{HCOCHO\cdots H_2O}$ complexes were fully optimized at M06-2X/6-311++G(3df, 3pd) level of theory in this study, and three different stable structures were obtained. Their optimized geometrical parameters and zero point vibrational energy corrected binding energies (BE) which are calculated by subtracting the total electronic energies of monomers forming the complex from the energy of that complex computed at CCSD(T)/6-311++G(3df, 3pd)//M06-2X/6-311++G(3df, 3pd) level are shown in Fig.2(a). Among

DOI:10.1063/1674-0068/29/cjcp1509193

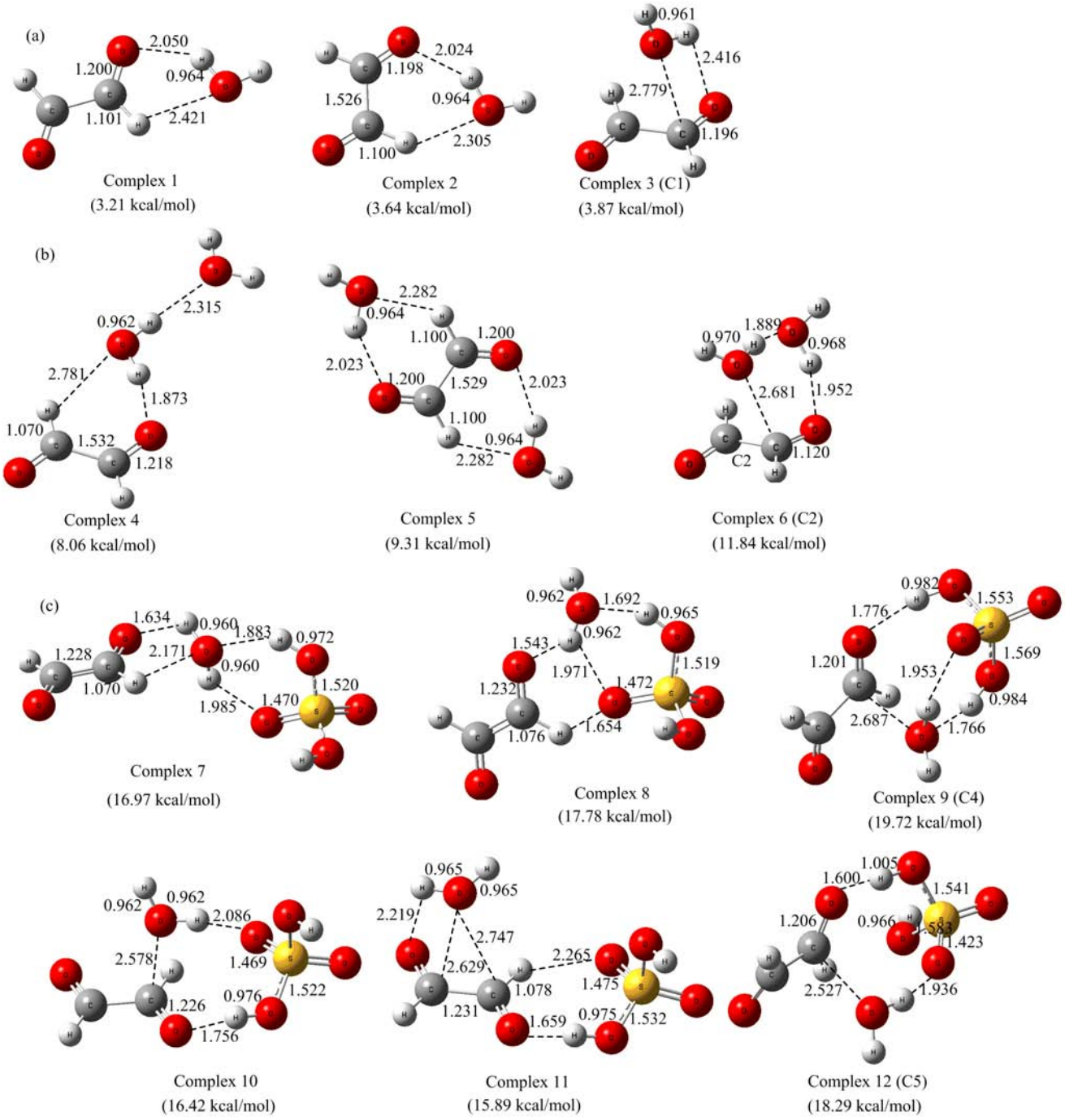

FIG. 2 (a) Three possible structures of the $HCOCHO\cdots H_2O$ complex, (b) three possible structures of the $HCOCHO\cdots H_2O\cdots H_2O$ complex, (c) six possible structures of the $HCOCHO\cdots H_2O\cdots H_2SO_4$ complex computed at the M06-2X/6-311++G(3df, 3pd) level (bond distances in Å). Their zero point corrected bonding energies (BE) are given in parentheses.

these three complexes, the geometries of complex 1 and 2 are near-planar whereas the geometry of complex 3 is nonplanar with respect to the glyoxal and water subunits forming the complex. As shown in Fig.2(a), the binding energies of these three complexes are comparable to each other, indicating that each complex might be expected to have roughly equal likelihood of contributing to the formation of the glyoxal-diol. However, we focus only on the complex 3 (labeled as C1), as the calculation result shows that complex 3 has the highest binding energy, and is the most stable complex.

It is worth noting that hydrolysis of the >C=O functional group of the glyoxal to form glyoxal-diol requires proper orientation of the water molecule with respect

DOI:10.1063/1674-0068/29/cjcp1509193

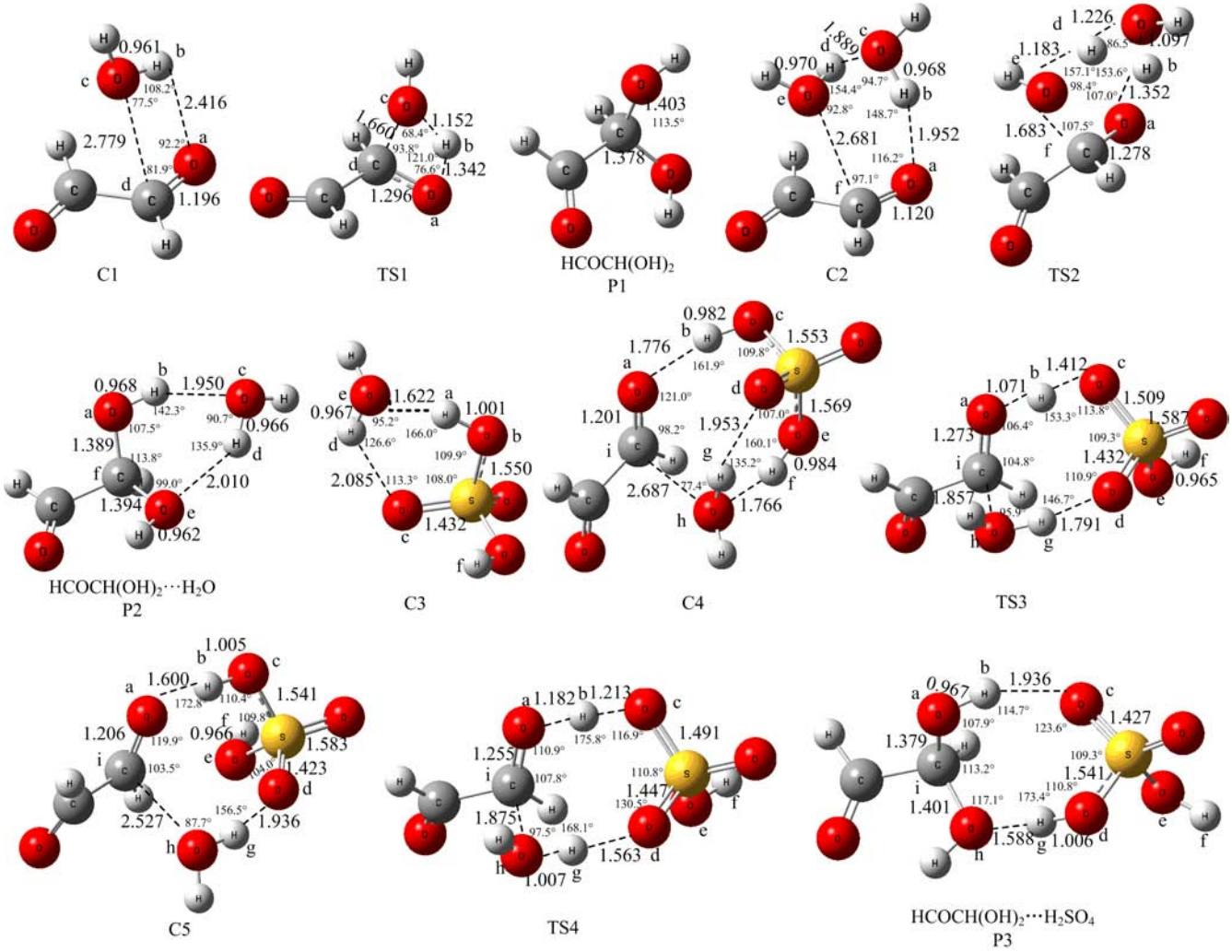

FIG. 3 Selected geometrical parameters of the optimized complexes, transition states and products at the M06-2X/6-311++G(3df, 3pd) level of theory (bond distances in Å and angles in (°)).

to >C=O functional group in the $HCOCHO\cdots H_2O$ complex, as this constraint is expected to minimize the barrier height. An orientation is considered favorable if it facilitates the simultaneous transfer of a hydrogen atom from the water molecule to the oxygen atom of the >C=O while the remaining OH moiety from the water molecule binds to the carbon atom of the >C=O through the formation of a C−O single bond. On the basis of the above considerations, complex 3 is seen to be more effective in promoting the hydrolysis reactions as it requires the least amount of reorientation compared to the other two complexes. Nonplanar complex 3 (C1) is a four-member ring structure with the bond distances of O_aH_b=2.416 Å, H_bO_c=0.961 Å, O_cC_d=2.779 Å, and C_dO_a=1.196 Å at the M06-2X/6-311++G(3df, 3pd) level of theory. C1 proceeds through the transition state TS1 to lead to the formation of glyoxal-diol (P1) as characterized in Fig.3. TS1 also involves a four-member ring cyclic transition state with the bond distances of O_aH_b=1.342 Å, H_bO_c=1.152 Å, O_cC_d=1.660 Å, and C_dO_a=1.296 Å. As shown in Fig.4, the barrier for the reaction, measured relative to C1 is 37.15 kcal/mol at CCSD(T)/6-311++G(3df, 3pd)//M06-2X/6-311++G(3df, 3pd) level of theory, which is so high that the process is impossible to occur in atmosphere.

When the gas phase hydrolysis of glyoxal involved two water molecules, the reactants are considered as either HCOCHO with the water dimer ($H_2O\cdots H_2O$) or $HCOCHO\cdots H_2O$ and water as follows:

$$\begin{aligned} HCOCHO + 2H_2O &\longleftrightarrow HCOCHO + H_2O\cdots H_2O \\ &\xleftarrow{K_{eq2}} HCOCHO\cdots H_2O\cdots H_2O(C2) \\ &\xrightarrow{k_{22}} HCOCH(OH)_2\cdots H_2O \\ &\longleftrightarrow HCOCH(OH)_2 + H_2O \qquad (2) \\ HCOCHO + 2H_2O &\rightleftharpoons HCOCHO\cdots H_2O + H_2O \\ &\xleftarrow{K_{eq3}} HCOCHO\cdots H_2O\cdots H_2O(C2) \end{aligned}$$

DOI:10.1063/1674-0068/29/cjcp1509193

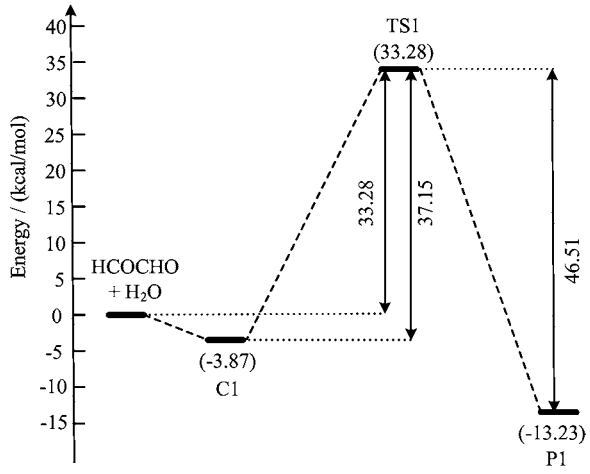

FIG. 4 Potential energy profile for the gas phase hydrolysis of HCOCHO involving a single water molecules at the CCSD(T)/6-311++G(3df, 3pd)//M06-2X/6-311++ G(3df, 3pd) level of theory.

$$\xrightarrow{k_{22}} \mathrm{HCOCH(OH)_2\cdots H_2O}$$
$$\longleftrightarrow \mathrm{HCOCH(OH)_2 + H_2O} \quad (3)$$

In enumerating the various possible trimeric complexes for Eq.(2) and Eq.(3), we have kept in mind that only orientations that will readily promote the formation of the glyxoal-diol through two simultaneous steps of hydrogen atom transfer and formation of a C−O bond between the water and glyxoal units will be important. Three different stable complexes which were fully optimized at M06-2X/6-311++G(3df, 3pd) are obtained and shown in Fig.2(b). It is noted that as the second water molecule is brought toward the $\mathrm{HCOCHO\cdots H_2O}$ complex, it can catalyze the hydrolysis reaction by acting either as a hydrogen atom acceptor (complex 4) or as a hydrogen atom donor (complex 5), or simultaneously as a hydrogen atom donor and acceptor (complex 6). Previous theoretical studies [18, 21] have found that only when the second water molecule acts as a bifunctional unit (*i.e.*, simultaneously acting as both a hydrogen atom donor and acceptor), is the reaction barrier significantly reduced relative to that involving hydrolysis by a single water molecule. Thus, complex 4 and complex 5 cannot compete with complex 6 with respect to their ability to reduce the reaction barrier. Also, the binding energy of complex 6 is 11.84 kcal/mol with respect to HCOCHO and two water molecules, higher than that of complex 4 and complex 5, respectively. Thus, complex 6 (labeled as C2 in Fig.3) was selected as the preferred $\mathrm{HCOCHO\cdots H_2O\cdots H_2O}$ complex for Eq.(2) and Eq.(3).

As displayed in Fig.3, the $\mathrm{HCOCHO\cdots H_2O\cdots H_2O}$ complex C2 involves $\mathrm{O_c{-}H_b\cdots O_a}$=1.952 Å and $\mathrm{O_e{-}H_d\cdots O_c}$=1.889 Å two weak hydrogen bonded interactions. The computed binding energy is 8.89 kcal/mol with respect to HCOCHO and water dimmer, and 7.97 kcal/mol with respect to $\mathrm{HCOCHO\cdots H_2O}$ dimmer and water at the CCSD(T)/6-311++G(3df, 3pd)//M06-2X/6-311++G(3df, 3pd) level of theory (Fig.5). The unimolecular isomerization of C2 to form $\mathrm{HCOCH(OH)_2\cdots H_2O}$ complex, via a six-member ring cyclic transition state TS2 with the bond distances of $\mathrm{O_aH_b}$=1.352 Å, $\mathrm{H_bO_c}$=1.097 Å, $\mathrm{O_cC_d}$=1.226 Å, $\mathrm{C_dO_e}$=1.183 Å, and $\mathrm{O_eC_f}$=1.683 Å at the M06-2X/6-311++G(3df, 3pd) level of theory. As can be seen from Fig.4 and Fig.5 that the activated barrier of HCOCHO with water dimer is reduced to 20.14 kcal/mol from 37.15 kcal/mol in the reaction $\mathrm{HCOCHO+H_2O}$ relative to the respective complexes, which agrees with the previous studies that the successive introduction of a second water molecule in the aldehyde hydrolysis reaction reduces the activation energy barrier for the unimolecular isomerization step [17–19]. However, the hydrolysis of glyoxal involving two water molecules is also not favored in the gas phase, as the barrier still remains prohibitive. In fact, Long *et al.* [18] and Hazra *et al.* [21] noted that even three water molecules are unable to reduce the barrier sufficiently to make the reaction feasible in the gas phase.

B. Hydrolysis of glyoxal catalyzed by sulfuric acid

The gas phase hydrolysis of glyoxal catalyzed by $\mathrm{H_2SO_4}$ (SA) can be considered in a manner analogous to that discussed above involving two water molecules:

$$\begin{aligned}&\mathrm{HCOCHO + H_2O + H_2SO_4}\\ &\quad\longleftrightarrow \mathrm{HCOCHO + H_2O\cdots H_2SO_4}\\ &\quad\xleftrightarrow{K_{\mathrm{eq4}}} \mathrm{HCOCHO\cdots H_2O\cdots H_2SO_4}\ \text{(C4)}\\ &\quad\xrightarrow{k_{23}} \mathrm{HCOCH(OH)_2\cdots H_2SO_4}\\ &\quad\longleftrightarrow \mathrm{HCOCH(OH)_2 + H_2SO_4} \quad (4)\\ &\mathrm{HCOCHO + H_2O + H_2SO_4}\\ &\quad\longleftrightarrow \mathrm{HCOCHO\cdots H_2O + H_2SO_4}\\ &\quad\xleftrightarrow{K_{\mathrm{eq4}}} \mathrm{HCOCHO\cdots H_2O\cdots H_2SO_4}\ \text{(C5)}\\ &\quad\xrightarrow{k_{23}} \mathrm{HCOCH(OH)_2\cdots H_2SO_4}\\ &\quad\longleftrightarrow \mathrm{HCOCH(OH)_2 + H_2SO_4} \quad (5)\end{aligned}$$

According to the theoretical calculation results of Torrent-Sucarrat *et al.* [22] and Long *et al.* [18], C3 has $\mathrm{O_b{-}H_a\cdots O_e}$=1.622 Å and $\mathrm{O_e{-}H_d\cdots O_c}$=2.085 Å two hydrogen bonded interactions, is the most stable $\mathrm{H_2SO_4\cdots H_2O}$ isomer. So, we consider the reactions of C3 with glyoxal and C1 with $\mathrm{H_2SO_4}$ for the gas phase hydrolysis of glyoxal catalyzed by SA. For the $\mathrm{HCOCHO+H_2SO_4\cdots H_2O}$ pathway, we began with the optimized geometry of glyoxal and then brought the $\mathrm{H_2SO_4\cdots H_2O}$ dimer, with its geometry fixed at its optimized value, toward the HCOCHO moiety to form

DOI:10.1063/1674-0068/29/cjcp1509193

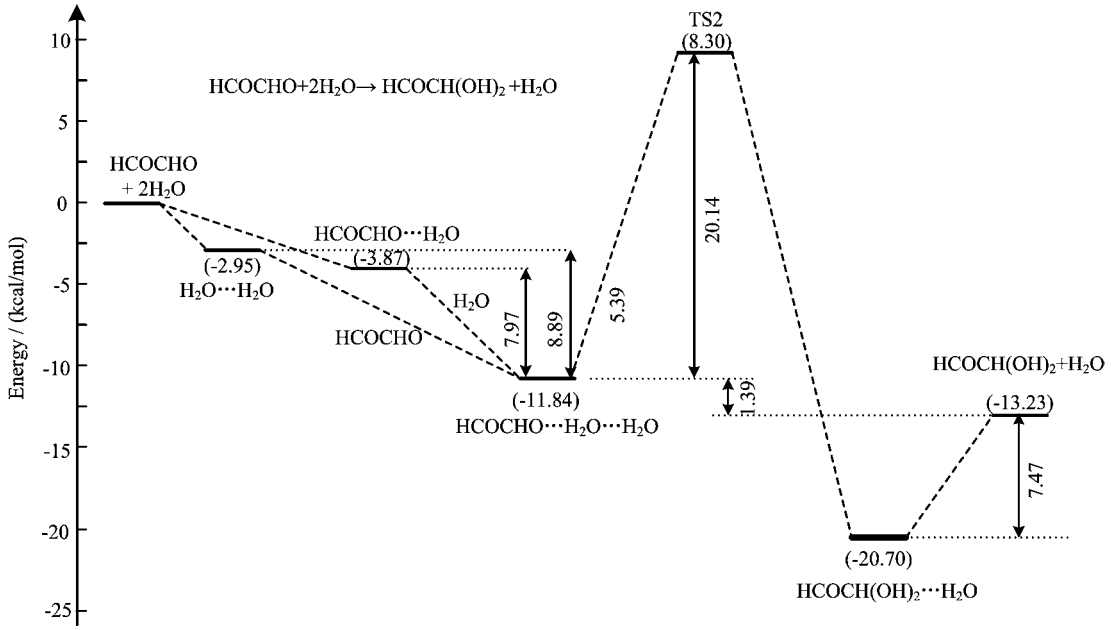

FIG. 5 Potential energy profile for the gas phase hydrolysis of HCOCHO involving two water molecules at the CCSD(T)/6-311++G(3df, 3pd)//M06-2X/6-311++G(3df, 3pd) level of theory (in kcal/mol).

possible geometries of the $HCOCHO\cdots H_2O\cdots SA$ preassociation complex. When the reactants are considered as C1 ($HCOCHO\cdots H_2O$) with H_2SO_4, we started with the optimized geometry of the C1 and then brought the H_2SO_4 moiety, at its isolated optimized geometry, toward the $HCOCHO\cdots H_2O$ dimer to form various possible structures for the preassociation complex.

Through this procedure a total of six different stable preassociation complex geometries were generated, and their optimized structures are shown in Fig.2(c) along with their binding energy computed at the M06-2X/6-311++G(3df, 3pd) level of theory. The first three geometries in Fig.2(c) are associated with the $HCOCHO+H_2SO_4\cdots H_2O$ channel, while the geometries represented by complex 10, complex 11, and complex 12 are associated with the $HCOCHO\cdots H_2O+H_2SO_4$ pathway. As noted earlier, efficient glyoxal-diol formation through glyoxal hydrolysis requires the formation of a C−O bond between the glyoxal and water moieties and the concomitant transfer of a hydrogen atom. From Fig.1(c) it is seen that among the structures shown complex 9 (labeled as C4 in Fig.3) and complex 12 (labeled as C5 in Fig.3) will be most effective in satisfying this requirement and reducing the reaction barrier. Also, our calculations found that the binding energy of complex 9 (C4 shown in Fig.3) is 19.72 kcal/mol relative to the reactants $H_2SO_4+H_2O+HCOCHO$, higher than that of complex 7 and complex 8, respectively, indicating that complex 9 (C4 shown in Fig.3), which has $O_c-H_b\cdots O_a$=1.776 Å, $O_e-H_f\cdots O_h$=1.766 Å and $O_h-H_g\cdots O_d$=1.953 Å three hydrogen bonded interactions, is the global minimum geometry of the $HCOCHO\cdots H_2O\cdots SA$ preassociation complex for the $HCOCHO+H_2SO_4\cdots H_2O$ pathway. Similarly, complex 12 (C5 shown in Fig.3), which possesses two hydrogen bonds $O_c-H_b\cdots O_a$=1.600 Å and $O_h-H_g\cdots O_d$=1.936 Å, and has the highest binding energy (18.29 kcal/mol relative to the reactants $H_2SO_4+H_2O+HCOCHO$), is the most stable complex when the reactants are considered as C1 ($HCOCHO\cdots H_2O$) with H_2SO_4. So, complex 9 (C4 shown in Fig.3) and complex 12 (C5 shown in Fig.3) were chosen as the preferred $HCOCHO\cdots H_2O\cdots SA$ complex for Eq.(4) and Eq.(5), respectively.

As indicated in Fig.6, the binding energy of C4 and C5 is 8.16 and 6.73 kcal/mol relative to the reactants C3+HCOCHO, respectively, indicating that C4 is more stable than C5. Further, our calculations show that the interconversion of the $HCOCHO\cdots H_2O\cdots SA$ preassociation complex from C4 to C5 via TS3 shown in Fig.2 with the barrier of about 2 kcal/mol. The preassociation complex C5 then undergoes the transition state TS4 and post-reactive complex P3 before the formation of H_2SO_4 and $HCOCH(OH)_2$, where the H_2SO_4 is acted as a catalyst. The TS4 with the bond distances of O_aH_b=1.182 Å, H_bO_c=1.213 Å, O_dH_g=1.563 Å, H_gO_h=1.007 Å, O_hC_i=1.875 Å and C_iO_a=1.255 Å is a concerted mechanism that the hydrogen atom H_b of OH group in H_2SO_4 is transferred to O_a in HCOCHO, the H_g atom of water is migrated to O_d in H_2SO_4, and simultaneously, the OH group in water is added to C_i in HCOCHO as characterized in TS4 of Fig.3. The calculated energy barrier is 7.08 kcal/mol with respect to C5 at the CCSD(T)/6-311++G(3df, 3pd)//M06-2X/6-311++G(3df, 3pd) level (Fig.6). These results

DOI:10.1063/1674-0068/29/cjcp1509193

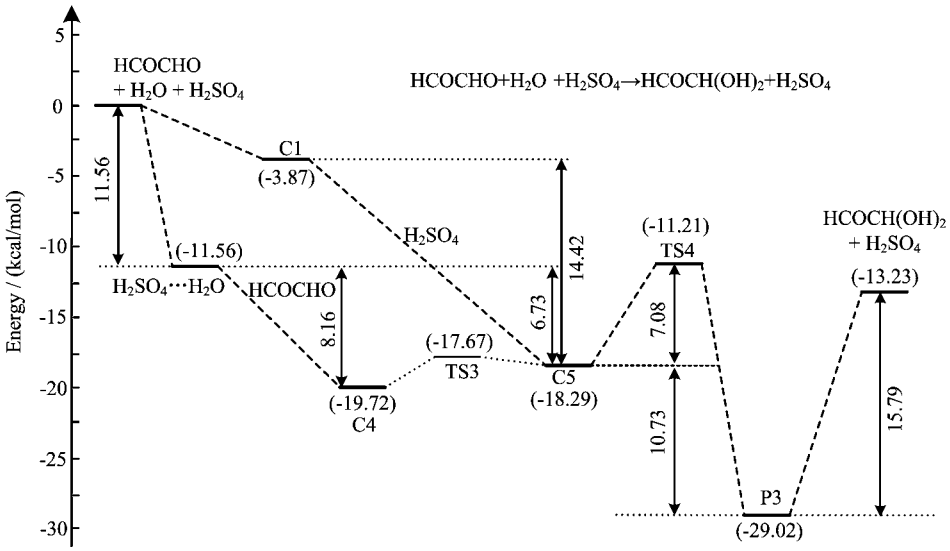

FIG. 6 Potential energy profile for the gas phase hydrolysis of HCOCHO catalyzed by H_2SO_4 at the CCSD(T)/6-311++G(3df, 3pd)//MX/6-311++G(3df, 3pd) level of theory (in kcal/mol).

show that the H_2SO_4 exerts a strong catalytic effect on the gas phase hydration of HCOCHO because the barrier is about 13 kcal/mol lower than the hydrolysis reaction involving two water molecules. It can be seen from the Fig.6 that the transition state barrier is only 0.35 kcal/mol above the energy of the HCOCHO+$H_2O\cdots H_2SO_4$ reactants. Therefore, the H_2SO_4 catalyzed reaction is expected to be an energetically favorable mechanism for the formation of glyoxal-diol in gas phase under atmospheric conditions.

It is worth noting that this acid catalysis mechanism differs from that normally associated with bulk aqueous phase acid-base chemistry and already known to be important in the atmosphere [37], in that no ions are involved in the reaction. It has generally been assumed in the literature that the hydrolysis reaction to produce the glyoxal-diol can only occur in the bulk aqueous phase due to the high barrier associated with the reaction. The present study finds that the relatively low barrier suggests that hydrolysis of glyoxal, and hence glyoxal-diol formation, can occur under water-restricted conditions with the aid of H_2SO_4. Examples of water-restricted environments where the present mechanism may be applicable to include low humidity gas phase reaction conditions such as that observed for the case of methyl glyoxal and ketene hydrolysis [38, 39], as well as reactions occurring on certain aerosol interfaces [40, 41].

C. Kinetic and applications in atmospheric chemistry

According to the above obtained activation energies, the conventional transition state theory and steady-state conditions, the rate constants for the gas phase hydrolysis of glyoxal are calculated. Five rate constant coefficients of Eq.(1) to Eq.(5) were determined using TheRate program 1.0 [36] in the 200−298 K temperature range. The computed data is shown in Table I. The kinetic data also demonstrates the conclusion that the reaction HCOCHO+H_2O is extremely minor in the gas phase because the rate constant is very low, about 10^{-41}−10^{-37} cm^3/(molecule·s) with the temperature range 200−298 K. For the reaction between HCOCHO and two waters, it is noted that the reported rate constant k_{tot3} for Eq.(3) is in the range of 1.45×10^{-25} cm^3/(molecule·s) to 5.15×10^{-24} cm^3/(molecule·s) at the temperature of 200−298 K, about twice higher than the rate constant k_{tot2} for Eq.(2). However, the rate constant k_{tot3} is still quite slow, is about 10^{-13} times lower than the rate constant of HCOCHO with OH by about 10^{-11} cm^3/(molecule·s) at the room temperature [5, 42, 43], which is minor in the atmosphere.

As for the H_2SO_4-catalyzed hydrolysis of glyoxal, contrast to other reported rate constant, k_{tot5} for Eq.(5) is inversely proportional to temperature, it is about 10^5 higher than the rate constant k_{tot4} for Eq.(4) at the temperature 200−298 K, showing a strong preference for the HCOCHO$\cdots H_2O$+SA pathway. The rate constant of the H_2SO_4 catalyzed hydrolysis of glyoxal is 1.34×10^{-11} cm^3/(molecule·s), about 10^{13} higher than that involving catalysis by an equal number of water molecules, and is greater than the reaction rate of glyoxal reaction with OH radicals of 1.10×10^{-11} cm^3/(molecule·s) at the room temperature [5, 42, 43]. The concentration of water [44] and H_2SO_4 [45] is 10^{11} and 10 higher than the concentration OH of about 10^6 molecules/cm^3, respectively, indicating that the gas phase hydrolysis of glyoxal of H_2SO_4 catalyst is feasible and could compete with the reaction glyoxal+OH under low humidity gas phase conditions, es-

DOI:10.1063/1674-0068/29/cjcp1509193

TABLE I The calculated equilibrium constant (K_{eq}), unimolecular rate constant (k_2, cm^3/(molecule·s)), and the total rate constant (k_{tot}, cm^3/(molecule·s)) for every elementary process for HCOCHO+H_2O, HCOCHO+$H_2O\cdots H_2O$, HCOCHO$\cdots H_2O$+H_2O, HCOCHO+$H_2O\cdots H_2SO_4$ and HCOCHO$\cdots H_2O$+H_2SO_4 reactions.

T/K	K_{eq1}	k_{21}	k_{tot1}	K_{eq2}	K_{eq3}	k_{22}	k_{tot2}
200	6.89×10^{-22}	8.26×10^{-20}	5.70×10^{-41}	2.28×10^{-18}	2.77×10^{-18}	5.26×10^{-8}	1.20×10^{-25}
220	2.84×10^{-22}	8.99×10^{-19}	2.55×10^{-40}	2.88×10^{-19}	3.97×10^{-19}	5.20×10^{-7}	1.50×10^{-25}
240	1.38×10^{-22}	1.08×10^{-17}	1.49×10^{-39}	5.21×10^{-20}	7.91×10^{-20}	5.19×10^{-6}	2.71×10^{-25}
260	7.58×10^{-23}	1.42×10^{-16}	1.07×10^{-38}	1.24×10^{-20}	2.04×10^{-20}	4.73×10^{-5}	5.86×10^{-25}
280	4.60×10^{-23}	2.00×10^{-15}	9.18×10^{-38}	3.64×10^{-21}	6.39×10^{-21}	3.68×10^{-4}	1.34×10^{-24}
298	3.14×10^{-23}	2.23×10^{-14}	6.99×10^{-37}	1.40×10^{-21}	2.59×10^{-21}	1.98×10^{-3}	2.79×10^{-24}
T/K	k_{tot3}	K_{eq4}	K_{eq5}	k_{23}	k_{tot4}	k_{tot5}	
200	1.45×10^{-25}	4.91×10^{-20}	5.97×10^{-13}	1.89×10^{4}	9.28×10^{-16}	1.13×10^{-8}	
220	2.06×10^{-25}	9.26×10^{-21}	2.27×10^{-14}	7.65×10^{4}	7.08×10^{-16}	1.74×10^{-9}	
240	4.11×10^{-25}	2.35×10^{-21}	1.50×10^{-15}	2.45×10^{5}	5.76×10^{-16}	3.68×10^{-10}	
260	1.09×10^{-24}	7.50×10^{-22}	1.52×10^{-16}	6.50×10^{5}	4.88×10^{-16}	9.88×10^{-11}	
280	2.35×10^{-24}	2.86×10^{-22}	2.16×10^{-17}	1.50×10^{6}	4.29×10^{-16}	3.24×10^{-11}	
298	5.15×10^{-24}	1.35×10^{-22}	4.68×10^{-18}	2.87×10^{6}	3.87×10^{-16}	1.34×10^{-11}	

Note: $k_{tot1}=K_{eq1}k_{21}$, $k_{tot2}=K_{eq2}k_{22}$, $k_{tot3}=K_{eq3}k_{22}$, $k_{tot4}=K_{eq4}k_{23}$, $k_{tot5}=K_{eq5}k_{23}$.

pecially at low temperature.

Due to high effective Henry's law constant, glyoxal is also scavenged by aqueous aerosol, fog, and cloud droplets in the atmosphere [7–10]. It is noted that when glyoxal is adsorbed onto the interface of an organic coated aerosol, in addition to heterogeneous reaction with OH radicals, the nominally hindered hydrolysis reactions can be facilitated on these water-restricted environments by the coadsorption of H_2SO_4 through the mechanism outlined above. The subsequent formation of glyoxal-diols and glyoxal dimmers, trimers and polymers species with their numerous OH groups and increased hydrogen bonding can then contribute toward the uptake of the glyoxal onto the aerosol even when they do not involve a liquid phase or bulk aqueous environment. On the other hand, these species are expected to result in significantly lower vapor pressure compared to the case for the parent glyoxal molecule; hence they are expected to partition more easily onto the particle phase and contribute to the growth of secondary organic aerosol. Thus, the present mechanism also provides a pathway for aerosol growth different from OH-initiated oxidation of glyoxal.

IV. CONCLUSION

The gas phase hydrolysis of glyoxal catalyzed by water and H_2SO_4 are theoretically investigated using the quantum chemical methods and the canonical transition state theory. The results suggest that H_2SO_4 shows a strong catalytic ability, which can significantly reduce the energy barrier for the hydration reaction of glyoxal. The transition state barrier is lowered to 7.08 kcal/mol from 37.15 kcal/mol relative to pre-reactive complexes at the CCSD(T)/6-311++G(3df, 3pd)//M06-2X/6-311++G(3df, 3pd) level of theory. The relatively low barrier suggests that this reaction mechanism can lead to facile formation of glyoxal-diol under low humidity gas phase conditions. The rate constant of the H_2SO_4 catalyzed hydrolysis of glyoxal is 1.34×10^{-11} cm^3/(molecule·s), which is greater than the reaction rate of glyoxal reaction with OH radicals at the room temperature, indicating that this process could compete with the reaction HCOCHO+OH under certain atmospheric conditions. This study may provide insight into how glyoxal-diol and other polymers species might be formed under atmospheric conditions associated with water-restricted environments and suggest that the formation of these precursors for secondary organic aerosol growth different from OH-initiated oxidation of glyoxal.

V. ACKNOWLEDGMENTS

This work is supported by the National Natural Science Foundation of China (No.41575118, No.41305109, No.21502086, No.41575126, No.41330424, and No.41127001), the Outstanding Youth Science Foundation of Fujian Province of China (No.2015J06009), and the Natural Science Foundation of Fujian Province of China (No.2015J05028). The author thanks professors W. T. Duncan, R. L. Bell, and T. N. Truong for providing TheRate programme through Internet.

[1] A. Karpfen, Comput. Theor. Chem. **1061**, 60 (2015).

DOI:10.1063/1674-0068/29/cjcp1509193

[2] S. Rossignol, K. Z. Aregahegn, L. Tinel, L. Fine, B. Nozière, and C. George, Environ. Sci. Technol. **48**, 3218 (2014).
[3] C. J. Kampf, R. Jakob, and T. Hoffmann, Atmos. Chem. Phys. **12**, 6323 (2012).
[4] M. Q. Huang, W. J. Zhang, Z. Y. Wang, L. Fang, R. H. Kong, X. B. Shan, F. Y. Liu, and L. S. Sheng, Chin. J. Chem. Phys. **24**, 672 (2011).
[5] J. Lockhart, M. Blitz, D. Heard, P. Seakins, and R. Shannon, J. Phys. Chem. A **117**, 11027 (2013).
[6] J. Tadic, G. K. Moortgat, and K. Wirtz, J. Photochem. Photobiol. A **177**, 116 (2006).
[7] T. Schaefer, D. van Pinxteren, and H. Herrmann, Environ. Sci. Technol. **49**, 343 (2015) .
[8] E. Avzianova and S. D. Brooks, Spectrochim. Acta A Mol. Biomol. Spectrosc. **101**, 40 (2013).
[9] D. J. Straub, J. W. Hutchings, and P. Herckes, Atmos. Environ. **47**, 195 (2012).
[10] A. K. Y. Lee, K. L. Hayden, P. Herckes, W. R. Leaitch, J. Liggio, A. M. Macdonald, and J. P. D. Abbatt, Atmos. Chem. Phys. **12**, 7103 (2012).
[11] M. E. Gomez, Y. Lin, S. Guo, and R. Zhang, J. Phys. Chem. A **119**, 4457 (2015).
[12] A. J. Sumner, J. L. Woo, and V. F. McNeill, Environ. Sci. Technol. **48**, 11919 (2014).
[13] A. K. Y. Lee, R. Zhao, R. Li, J. Liggio, S. M. Li, and J. P. D. Abbatt, Environ. Sci. Technol. **47**, 12819 (2013).
[14] M. Kalberer, D. Paulsen, M. Sax, M. Steinbacher, J. Dommen, A. S. H. Prevot, R. Fisseha, E. Weingartner, V. Frankevich, R. Zenobi, and U. Baltensperger, Science **303**, 1659 (2004).
[15] S. Wolfe, C. K. Kim, K. Yang, N. Weinberg, and Z. Shi, J. Am. Chem. Soc. **117**, 4240 (1995).
[16] S. Boöhm, D. Antipova, and J. Kuthan, Int. J. Quantum Chem. **58**, 47 (1996).
[17] J. Kua, S. W. Hanley, and D. O. De Haan, J. Phys. Chem. A **112**, 66 (2008).
[18] B. Long, X. F. Tan, C. R. Chang, W. X. Zhao, Z. W. Long, D. S. Ren, and W. J. Zhang, J. Phys. Chem. A **117**, 5106 (2013).
[19] M. K. Hazra, J. S. Francisco, and A. Sinha, J. Phys. Chem. A **117**, 11704 (2013).
[20] L. Vereeckenand J. S. Francisco, Chem. Soc. Rev. **41**, 6259 (2012).
[21] M. K. Hazra, J. S. Francisco, and A. Sinha, J. Phys. Chem. A **118**, 4095 (2014).
[22] M. Torrent-Sucarrat, J. S. Francisco, and J. M. Anglada, J. Am. Chem. Soc. **134**, 20632 (2012).
[23] M. Sipilä, T. Berndt, T. Petäjä, D. Brus, J. Vanhanen, F. Stratmann, J. Patokoski, R. L. Mauldin, A. P. Hyvärinen, H. Lihavainen, and M. Kulmala, Science **327**, 1243 (2010).
[24] J. Elm, M. Bilde, and K. V. Mikkelsen, J. Chem. Theory Comput. **8**, 2071 (2012).
[25] M. J. Frisch, G. W. Trucks, H. B. Schlegel, G. E. Scuseria, M. A. Robb, J. R. Cheeseman, G. Scalmani, V. Barone, B. Mennucci, G. A. Petersson, H. Nakatsuji, M. Caricato, X. Li, H. P. Hratchian, A. F. Izmaylov, J. Bloino, G. Zheng, J. L. Sonnenberg, M. Hada, M. Ehara, K. Toyota, R. Fukuda, J. Hasegawa, M. Ishida, T. Nakajima, Y. Honda, O. Kitao, H. Nakai, T. Vreven, J. A. Montgomery Jr., J. E. Peralta, F. Ogliaro, M. Bearpark, J. J. Heyd, E. Brothers, K. N. Kudin, V. N. Staroverov, R. Kobayashi, J. Normand, K. Raghavachari, A. Rendell, J. C. Burant, S. S. Iyengar, J. Tomasi, M. Cossi, N. Rega, J. M. Millam, M. Klene, J. E. Knox, J. B. Cross, V. Bakken, C. Adamo, J. Jaramillo, R. Gomperts, R. E. Stratmann, O. Yazyev, A. J. Austin, R. Cammi, C. Pomelli, J. W. Ochterski, R. L. Martin, K. Morokuma, V. G. Zakrzewski, G. A.Voth, P. Salvador, J. J. Dannenberg, S. Dapprich, A. D. Daniels, Ö. Farkas, J. B. Foresman, J. V. Ortiz, J. Cioslowski, and D. J. Fox, *Gaussian 09 Revision*, Wallingford CT: Gaussian, Inc., (2009).
[26] K. Fukui, Acc. Chem. Res. **14**, 363 (1981).
[27] G. D. Purvis Iii and R. J. Bartlett, J. Chem. Phys. **76**, 1910 (1982).
[28] Y. P. Liu, G. C. Lynch, T. N. Truong, D. H. Lu, D. G. Truhlar, and B. C. Garrett, J. Am. Chem. Soc. **115**, 2408 (1993).
[29] C. Gonzalez and H. B. Schlegel, J. Phys. Chem. **94**, 5523 (1990).
[30] D. G. Truhlar and B. C. Garrett, Ann. Rev. Phys. Chem. **35**, 159 (1984).
[31] J. C. Keck, J. Chem. Phys. **32**, 1035 (1960).
[32] C. Eckart, Phys. Rev. **35**, 1303 (1930).
[33] M. Q. Huang, Y. M. Liao, Z. Y. Wang, L. Q. Hao, and W. J. Zhang, Comput. Theor. Chem. **1037**, 63 (2014).
[34] M. Q. Huang, Z. Y. Wang, L. Q. Hao, and W. J. Zhang, Comput. Theor. Chem. **996**, 44 (2012).
[35] V. H. Uc, J. R. Alvarez-Idaboy, A. Galano, I. Garcia-Cruz, and A. Vivier-Bunge, J. Phys. Chem. A **110**, 10155 (2006).
[36] S. Zhang and T. N. Truong, *VKLab Version 1.0*, Salt Lake City USA: University of Utah, (2001).
[37] M. Jang, N. M. Czoschke, S. Lee, and R. M. Kamens, Science **298**, 814 (2002).
[38] J. L. Axson, K. Takahashi, D. O. De Haan, and V. Vaida, Proc. Natl. Acad. Sci. USA **107**, 6687 (2010).
[39] T. F. Kahan, T. K. Ormond, G. B. Ellison, and V. Vaida, Chem. Phys. Lett. **565**, 1 (2013).
[40] D. J. Donaldson and V. Vaida, Chem. Rev. **106**, 1445 (2006).
[41] D. Clifford, T. Bartel-Rausch, and D. J. Donaldson, Phys. Chem. Chem. Phys. **9**, 1362 (2007).
[42] K. J. Feierabend, L. Zhu, R. K. Talukdar, and J. B. Burkholder, J. Phys. Chem. A **112**, 73 (2007).
[43] C. N. Plum, E. Sanhueza, R. Atkinson, W. P. L. Carter, and J. N. Pitts, J. Environ. Sci. Technol. **17**, 479 (1983).
[44] A. Galano, M. Narciso-Lopez, and M. Francisco-Marquez, J. Phys. Chem. A **114**, 5796 (2010).
[45] T. Petäjä, R. L. III Mauldin, E. Kosciuch, J. McGrath, T. Nieminen, P. Paasonen, M. Boy, A. Adamov, T. Kotiaho, and M. Kulmala, Atmos. Chem. Phys. **9**, 7435 (2009).

DOI:10.1063/1674-0068/29/cjcp1509193